Journal of Fluorescence, Vol. 15, No. 5, September 2005 (© 2005)
DOI: 10.1007/s10895-005-2986-4

The Anthracen-9-ylmethyloxy Unit: An Underperforming Motif Within the Fluorescent PET (Photoinduced Electron Transfer) Sensing Framework

David C. Magri,[1] John F. Callan,[1,2] A. Prasanna de Silva,[1,5] David B. Fox,[1] Nathan D. McClenaghan,[3] and K. R. A. Samankumara Sandanayake[4]

Received June 10, 2005; accepted July 19, 2005

Compound **2**, which was designed to act as a fluorescent sensor for calcium according to the PET (Photoinduced Electron Transfer) principle, shows a relatively small Ca^{2+}-induced fluorescence enhancement factor (FE) of 1.8 whereas its close relative **1** is known to display a far higher FE value of 16. Though designed as fluorescent PET sensors for solvent polarity, compounds **5** and **6** also show negligible fluorescence enhancement as their environments are made progressively less polar even though their relatives **3** and **4** show limiting FE values of 53 and 3, respectively. Indeed, **3** and **4** are useful since they are fluorescent sensors for solvent polarity without being affected by Bronsted acidity. The poor sensory performance of **2**, **5,** and **6** relative to their cousins is attributed to the presence of an oxygen proximal to the 9-position of an anthracene unit, which opens up a CT (charge transfer) channel. Normal PET sensing service is resumed when the offending oxygen is deleted.

KEY WORDS: Fluorescent sensors; ion sensors; polarity sensors; PET; electron transfer.

INTRODUCTION

Since its generalization over a decade ago [1–3], the fluorescent PET (Photoinduced Electron Transfer) sensing principle involving "fluorophore-spacer-receptor" systems is now producing useful examples with regular frequency [4]. The scientific simplicity of the principle has remained its most endearing and applicable feature. Its simplest and most popular manifestation engages an aliphatic amine as an electron donor and as a receptor for the cation being sensed. The PET path clearly originates at the nitrogen lone electron pair and terminates at the fluorophore. However, various other electron donors can be similarly engaged, provided that basic conditions are met (see later). Many of these electron donors are polyatomic π-systems where an atomic origin for the PET process cannot be pinpointed. For convenience, the spacer can be taken to be the σ-bond set between where the π-system of the electron donor ends and where the π-system of the fluorophore begins. We stress that the fluorescent PET sensing principle is powerful because it is not restricted to a few chemical/structural motifs. Nevertheless, we can expect that limitations of the entry-level model of the fluorescent PET sensing principle (like all such models) will emerge from time to time as more and more specific examples, each with its structural peculiarities, are examined. Safeguards can then be added to the simple model to keep the principle as a whole as strong and predictive as before. For instance, a strong regioselectivity of sensory behavior was found concerning the point of attachment of "receptor–spacer" assemblies to fluorophores. The regioselection was so strong as to destroy the sensing action in some cases [5]. This was traced to a molecular-scale electric field naturally photogenerated

[1] School of Chemistry, Queen's University, Belfast, Northern Ireland.
[2] School of Pharmacy, Robert Gordon University, Aberdeen, Scotland.
[3] Laboratoire de Chimie Organique et Organométallique, UMR 5802 CNRS, Universite Bordeaux 1, Talence, France.
[4] Phosphagenics R&D Laboratory, Department of Biochemistry and Molecular Biology, Monash University, Victoria, Australia.
[5] To whom correspondence should be addressed. E-mail: a.desilva@qub.ac.uk

[5a,6] in ICT(internal charge transfer)/PCT(photoinduced charge transfer) [2h,3e] excited states, as well as the presence of a frontier orbital node at certain positions of this particular fluorophore [6,7]. Now we find another rather simple structural motif, which throws up sensory weaknesses which are understandable and avoidable in subsequent PET sensor designs.

A particular flexibility of the PET sensor principle has been its capability of sensing some physicochemical properties such as solvent polarity [8,9] besides a whole variety of chemical species [2]. We now consider the above-mentioned sensory weakness in both these contexts.

EXPERIMENTAL

UV-visible absorption and fluorescence emission spectra were recorded on Perkin-Elmer Lambda 9 and Perkin-Elmer LS-5B instruments. A General Electric GN500 nuclear magnetic resonance spectrometer and VG MS902 mass spectrometer were also employed. The experimental procedure for the preparation of **1** is in Ref. [10]. The preparative procedure for **3** and **4** are in Ref. [8]. The syntheses for 2[[bold]], 5[[bold]] and 6[[bold]] are listed below.

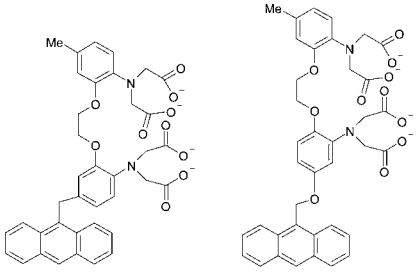

2-[5-(9-Anthrylmethoxy)(Carboxymethyl)-2-(2-{2-[Di(Carboxymethyl)Amino]-5-Methylphenoxy}Ethoxy)Anilino]Acetic Acid (2)

The tetramethyl ester of the oxyBAPTA receptor [11] (0.23 g), 9-(bromomethyl)anthracene [12] (0.12 g), 18-crown-6 (0.43 g), and anhydrous potassium carbonate (0.11 g) were suspended in dry acetonitrile (20 mL). After flushing the system for several minutes with nitrogen, this was refluxed under a nitrogen atmosphere for 12 hr. The crude reaction mixture was then evaporated to dryness, dissolved in dichloromethane (25 mL), and washed three times with 0.5 M aqueous KCl solution (10 mL) and finally with water. The organic phase was then dried over anhydrous sodium sulfate and the solvent removed to yield a yellow residue. Purification was further achieved using flash silica column chromatography, eluting with dichloromethane:methanol – 96:4 v/v. Evaporation of solvent then gave the product as a yellow-brown gummy solid (68% yield). pmr δ, ($CDCl_3$) 8.51(s, 1H, Anth$-H$), 8.28(d, 2H, $J = 8$ Hz, Anth$-H$), 8.04(d, 2H, $J = 8$ Hz, Anth$-H$), 7.48–7.54(m, 4H, Anth$-H$), 6.88(d, 1H, $J = 8$ Hz, Ar$-H$), 6.68–6.77(m, 2H, Ar$-H$), 6.58(s, 2H, Ar$-H$), 6.52(d, 1H, $J = 3$ Hz, Ar$-H$), 5.88(s, 2H, Anth$-CH_2-$), 4.26(s, 4H, O$-CH_2-$), 4.15(s, 4H, N$-CH_2-$), 4.14(s, 4H, N$-CH_2-$), 3.61(s, 6H, O$-CH_3$), 3.54(s, 6H, O$-CH_3$), 2.28 (s, 3H, Ar$-CH_3$). *m/z* (%)(ES): 753(M^+, 45), 776($M + Na^+$, 100), 563(6), 334(67). $ir_{\nu max}$(KBr) 3040, 2940, 1875, 1552, 918, 861, 770, 674, 642, 596 cm^{-1}.

The previous compound (27 mg) was dissolved in THF and potassium hydroxide (5 equivalents) was added in aqueous solution. This was then heated and methanol was added until a homogeneous solution was obtained. After refluxing for 90 min, the solvents were removed under reduced pressure, yielding a yellow gum. pmr δ, (D_2O) 8.33(s, 1H, Anth$-H$), 8.08(d, 2H, $J = 8$ Hz, Anth$-H$), 7.90(d, 2H, $J = 8$ Hz, Anth$-H$), 7.39(m, 4H, Anth$-H$), 6.84–6.90 (m, 2H, Ar$-H$), 6.73(s, 2H, Ar$-H$), 6.47–6.53(m, 2H, Ar$-H$), 5.60(s, 2H, Anth$-CH_2-$), 4.17(br.s, 4H, O$-CH_2-$), 3.77(br.s, 8H,N$-CH_2-$), 2.21 (s, 3H, Ar$-CH_3$).

Preparation of 10-[(4-Methoxyphenoxy)Methyl]-9-Anthracenecarbonitrile (5)

9-bromomethyl-10-cyanoanthracene [13] (0.3 g, 1.01 mmol) was dissolved under reflux in acetone (30 mL) in a 100 mL round bottom flask fitted with condenser and drying tube. After cooling to room temperature 4-methoxyphenol (0.124 g, 1mmol), anhydrous potassium carbonate (0.138 g, 1 mmol), 18-crown-6 (0.53 g,

2 mmol), and acetone (40 mL) were added. This was allowed to reflux for 8 hr. After cooling to room temperature the solvent was removed by evaporation. The crude product was shaken in water and filtered. The product was then recrystallized from hot ethanol to yield **5** as a yellow solid (85% yield), m.p. 199–200°C. pmr δ, ($CDCl_3$): 8.51 (d, 2H, $J = 8.7$ Hz, Anth−*H*), 8.39 (d, 2H, $J = 8.9$ Hz, Anth−*H*), 7.70 (m, 4H, $J = 5.5$ Hz, Anth−H), 7.05 (d, 2H, $J = 9.1$ Hz, Ph−*H*), 6.91 (d, 2H, $J = 9.1$ Hz, Ph−*H*), 5.93 (s, 2H, Anth−CH_2−O), 3.82 (s, 3H, O−CH_3). *m/z* (%) (EI): 339.1260 (expected 339.1259). ir$_{\nu max}$(KBr) 3030, 2900, 2216, 1511, 1226, 1032, 753, 739 cm^{-1}.

Preparation of 10-[(3,4-Dimethoxyphenoxy)Methyl]-9-Anthracenecarbonitrile (6)

The preparation of **6** was obtained by the same procedure as **5**, except substituting 4-methoxyphenol with 3,4-dimethoxyphenol. Compound **6** was isolated as a pale yellow/green solid (63% yield). m.p. 206–207°C. pmr δ, ($CDCl_3$): 8.42 (dd, 4H, $J = 7$ Hz, 30 Hz, Anth−*H*), 7.69 (dtd, 4H, $J = 1$ Hz, 7 Hz, 30 Hz, Anth−H), 6.89 (d, 1H, $J = 9$ Hz, Ph−*H*), 6.72 (dd, 1H, $J = 2$ Hz, 9 Hz Ph−*H*), 6.60 (d, 1H, $J = 2$ Hz, Ph−*H*), 5.92 (s, 2H, Anth−CH_2−O), 3.89 (s, 3H, −OCH_3), 3.81 (s, 3H, O−CH_3). *m/z* (%)(EI): = 369.1369 (Expected 369.1365). ir$_{\nu max}$(KBr) 3026, 2850, 2500, 2218, 1596, 1514,1442, 1386,1278, 1025, 745 cm^{-1}.

RESULTS AND DISCUSSION

PET Sensor for Ca^{2+}

We previously incorporated Tsien's BAPTA Ca^{2+}-receptor [11,14] into PET sensor **1** by employing it as an electron donor [10] where electron transfer to an excited fluorophore serves to quench the fluorescence emission. Binding Ca^{2+} to **1** results in a restoration of fluorescence emission of the anthracene unit as this quenching channel is blocked. **1** conforms to the "fluorophore—spacer–receptor" format, where a single methylene unit effectively segregates the two π-systems. We note that the electron donor within **1** is the oxyaniline moiety rather than a simple amine.

While sensor **1** works very well, its synthesis has a weakness. The crucial coupling of the BAPTA receptor (in the form of its tetramethyl methyl ester) to the fluorophore–spacer assembly requires a mild Friedel–Crafts procedure that is quite poor-yielding. So we were attracted to sensor **2**, which achieves the coupling via a simple, high-yielding nucleophilic substitution reaction of 9-(bromomethyl)anthracene [12] with the known tetramethyl ester of the oxyBAPTA receptor [11]. Sensor **2** differs from **1** mainly in the insertion of an additional oxygen atom between the spacer and the donor. We note that the spacer is still a methylene unit, since the additional oxygen atom is conjugated with the oxyaniline electron donor. In other words, the electron donor within **2** is a dioxyaniline unit. The different position of fluorophore attachment to the receptor is considered to be of lesser consequence for the comparative behavior of **1** and **2**. Variation of the position of attachment of pyridine receptors in PET systems has no significant effect on sensor action [15]. Therefore, the effect of incorporation of this additional oxygen atom can be determined by comparing the fluorescence properties of these molecules.

Since the spacer is a single methylene unit in both **1** and **2**, any differential fluorescent sensing behavior cannot be viewed in terms of increased distance between the fluorophore and the receptor upon addition of the new oxygen atom to "mutate" **1** into **2**. We stress this point because the fall-off of PET rates with increasing distance [3e] is very well appreciated. As we consider the results of this work, the distance dependence of PET needs to be eliminated as a possible suspect from our inquiry at this early stage itself. We proceed on this basis.

UV-Visible Spectroscopic Response of 2 to Ca^{2+}

It is well-appreciated that PET sensors will not show any serious ion-induced changes in the fluorophore's lowest energy absorption band [2b]. Only subtle changes are seen in the lower energy features on varying the concentration of Ca^{2+} at a pH value of 7.2 (Fig. 1). Larger changes are observed in the higher energy feature associated with the *N*,*N*-dialkylanilino moiety which is blue-shifted out of the range of monitoring. Analysis of the absorbance (A) changes in this region (e.g., at 312 nm) as a function of Ca^{2+}-concentration according to Eq. (1) [10,15] yields the ground state binding constant (log β value) of 6.9. The reason for the alteration of the anilino band is the Ca^{2+}-induced decoupling of the amine electron pair from the dioxyphenyl unit.

$$\log\left[\frac{(A_{max} - A)}{(A - A_{min})}\right] = \text{pCa} - \log\,\beta \qquad (1)$$

Fluorescence Spectroscopic Response of 2 to Ca^{2+}

The emission output from sensor **2** as a function of the Ca^{2+} concentration is shown in Fig. 2. Unlike **1**, this sensor exhibits a small fluorescence enhancement of 1.8 on binding Ca^{2+}. Additionally, the quantum yield is

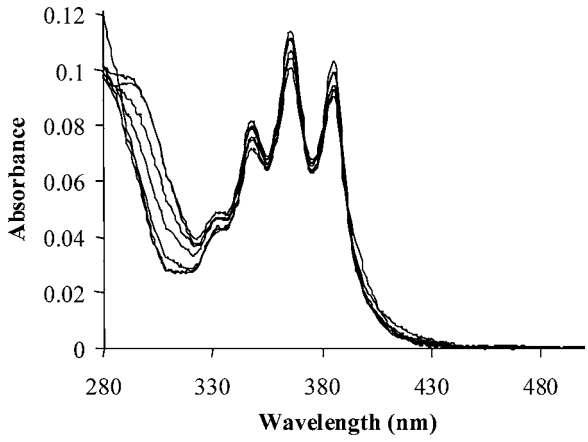

Fig. 1. Overlaid absorption spectra of **2** on varying pCa (pH =7.2). pCa values in the order of increasing absorbance at 312 nm; 2.3, 6.0, 6.5, 7.0, 7.5, 8.0, and ∞.

found to be significantly lower ($\Phi_{\text{Flu.max}} = 0.010$ compared with 0.023). These and other comparative parameters are shown in Table I. Analysis of the ϕ_{Flu} – pCa profile according to Eq. (2) [10,15] yields the log β value of 6.5.

$$\log\left[\frac{(\phi_{\text{Flu. max}} - \phi_{\text{Flu}})}{(\phi_{\text{Flu}} - \phi_{\text{Flu. min}})}\right] = \text{pCa} - \log\,\beta \qquad (2)$$

The fluorescence response of **1** to other larger divalent ions is also included in Table I. Indeed, the ability of the BAPTA receptor to bind these ions has been reported [16,17]. Binding of the posttransition ion Zn^{2+} results in the highest fluorescence enhancement because of the drainage of electrons from the receptor toward the formation of a coordinate bond with covalent character, in addition to the usual deconjugation resulting from the conformational change of the receptor [10]. The smaller

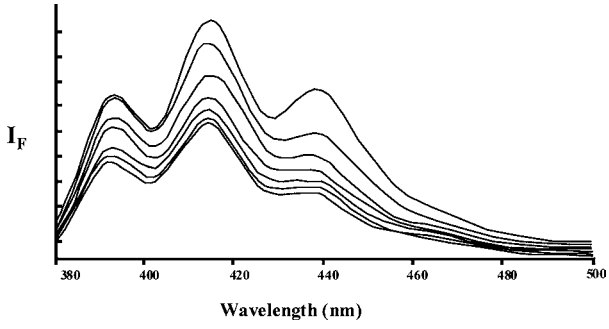

Fig. 2. Overlaid emission spectra of **2** on varying pCa (pH = 7.2). pCa values in order of increasing emission intensity at 414 nm; 2.3, 6.0, 6.5, 7.0, 7.5, 8.0, and ∞.

Table I. Comparative Coordination and Optical Properties of **1** and **2**[a]

Property	**1**	**2**
ΔG_{PET}/kJmol^{-1}	−23	≤23
λ_{abs}/nm	390, 368, 352	386, 367, 349
ε_{max}/mol^{-1} dm^3 cm^{-1}	8100, 8300, 5400	8400, 8700, 5600
λ_{exc}/nm	368	372
λ_{flu}/nm	394, 416, 440	393, 414, 438
$\phi_{\text{flu.max}}$[b]	0.023	0.010
$\phi_{\text{flu.min}}$[c]	0.0014	0.005
log $\beta_{Ca^{2+}}$	6.6	6.5(6.9)[d]
$FE_{Ca^{2+}}$	16	1.8

[a] 10^{-5} M **1** and **2** in water at pH =7.2, $I = 0.1$ M(KCl).
[b] At pCa = 2.3. Zn^{2+}, Sr^{2+}, and Ba^{2+} at given corresponding values of 0.035, 0.010, and 0.006, respectively.
[c] At pCa = ∞.
[d] By measuring absorbance changes at 312 nm.

effects of the two larger alkaline earth ions suggest their inability to fit into the BAPTA cavity.

The thermodynamics of PET (ΔG_{PET}) can be estimated according to the Weller equation (3) [18] along with available electrochemical data [19a].

$$\Delta G_{\text{PET}} = -E_{\text{S}} - E_{\text{red.fluo}} + E_{\text{ox.donor}} - \frac{e^2}{\varepsilon r} \qquad (3)$$

where E_{S} and $E_{\text{red.fluo}}$ are the singlet energy and the reduction potential of the fluorophore, respectively, $E_{\text{ox.donor}}$ is the oxidation potential of the electron donor unit, which is an oxyaniline for **1** and a dioxyaniline for **2**. The ion-paring term $e^2/\varepsilon r$ is 10 kJ mol^{-1} in acetonitrile [19b]. The ΔG_{PET} values (estimated in acetonitrile) for **1** and **2** are given in Table I. Unfortunately, the corresponding values for water solvent are not available. It is clear that the thermodynamic driving force for PET is more favorable for Ca^{2+}-free **2** *c.f.* Ca^{2+}-free **1**, though the fluorescence quantum yield($\phi_{\text{Flu.min}}$) is higher for **2**. This could also suggest the possibility of a residual PET process in the Ca^{2+}-bound **2**, which can lower the fluorescence quantum yield ($\phi_{\text{Flu.max}}$). Such residual PET processes have been observed in some Ba^{2+}-bound crown ether sensors by Nagamura and his coworkers [20]. However, the Ca^{2+}-induced decoupling [10] of the amine electron pair from the dioxyphenyl unit should minimize any residual PET in the case of Ca^{2+}-bound **2**.

So we need to look elsewhere for the reason why the sensory performance of **2** is poor in terms of both the Ca^{2+}-induced fluorescence enhancement factor and the quantum yield in the Ca^{2+}-bound state ($\phi_{\text{Flu.max}}$). It has been known for sometime that 9-alkoxy/hydroxymethyl anthracene has a low quantum yield [21,22]. Although detailed analyses have not been conducted for this phenomenon, Desvergne *et al.* have suggested it to be due to a CT (charge transfer) interaction between the excited

anthracene acting as an acceptor and the proximal oxygen acting as a donor [23]. In fact the importance of the electron-rich oxygen has been clearly demonstrated by structural variations [22]. Such a CT interaction would be preserved in **2** even though the electron-rich aryloxy nature of the proximal oxygen will create the PET channel discussed in the previous paragraph. The coexistence of two deexcitation pathways is accommodated by the two electron pairs on the proximal oxygen. Ca^{2+}-binding to **2** would restrain the PET process but the large distance of the Ca^{2+} centre from the proximal oxygen would still leave the CT channel open for deexcitation, albeit less efficient. Hence the $\phi_{Flu.max}$ value of **2** remains small.

PET Sensors for Solvent Polarity

Perhaps the most convenient and best-known method for measuring solvent polarity is based on the $E_T(30)$ scale [24], which uses the ICT absorption band maximum of a pyridinium phenol betaine. Related fluorescence-based methods [25] are also available. A weakness of all these methods is the inability to evaluate individual contributions from the dipolarity (π^*), hydrogen bond acidity (α), or basicity (β) of the solvent [26]. An approach, based on specific examples involving ICT or related mechanisms, has been developed by Taft and coworkers [26] to overcome these shortfalls. We have previously found this approach to be useful [27].

PET sensors for solvent polarity are relative newcomers to this field and normally include a methylene unit as the spacer and an amine functionality as the electron donor [8]. Briefly, PET in neutral molecules generates a radical ion pair. The latter is preferentially stabilized in solvents with dipoles and hydrogen bonding sites. Therefore, the PET rate is accelerated in such solvents and the fluorescence quantum yield (ϕ_{Flu}) falls concurrently. These systems show excellent switching "on" of the fluorescence quantum yield in less polar solvents describable by Eq. (4), if protic solvents were excluded [8]. Equation (4) is for solvent polarity sensors what Eq. (2) is for metal ion sensors. The spectral parameters other than ϕ_{Flu} remain virtually unaffected.

$$\log[(\phi_{Flu.max}/\phi_{Flu}) - 1] = A(\pi * + k\beta) + C \qquad (4)$$

The mixing coefficient k was determined by the best fit of the experimental data to Eq. (4) and is expected to be nonzero if hydrogen bonding occurs from the sensor to the solvent during the sensing process. A and C are constants. A weakness, however, is that trace acids present in solvents can protonate the amine group, raise the oxidation potential of the donor, and inhibit PET. The necessity for rigorous purification of the solvents prior to use reduces the effectiveness of this type of probe. In order to construct sensors that would not act as Bronsted bases, the amine-free derivatives **3**–**6** were prepared and assessed. If successful, these would be quite important since fluorescent sensors for solvent polarity, which are based on amine-free structures, are rare [25a,28].

Compound **3** has a 9-cyanoanthracene fluorophore and an oxyphenyl electron donor, whereas compound **4** possesses a dioxyphenyl electron donor. Again, cases **5** and **6** are "mutants" obtained by inserting an additional oxygen atom into **3** and **4,** respectively, so that the electron donor is extended. It may be noted that the oxyphenyl electron donor in **3** has been extended by one oxygen atom in two different ways in the cases of compounds **4** and **5**. Of course, there is no receptor requirement in sensors for polarity. The spacer in all these four cases is a single methylene unit. The commentary made earlier for the Ca^{2+} sensors also applies here.

Thermodynamic calculations for PET using the Weller equation [18] (along with available electrochemical data) [19a] suggest that both **4** and **5** should be responsive to changes in solvent polarity, having small ΔG_{PET} values (-11 and $-22\,kJ\,mol^{-1}$, respectively). The stabilization offered from a solvent to the radical ion pair formed after a PET process involving a neutral molecule, decreases with decreasing solvent polarity. This can be sufficient to overturn these small ΔG_{PET} values for **4** and **5** to make the PET process endergonic. So the fluorescence becomes switched "on." Compound **3** with its more positive ΔG_{PET} values ($+19\,kJ\,mol^{-1}$) is only expected to be switched "off" with regard to its fluorescence in solvents much more polar than acetonitrile. Compound **6**, with a ΔG_{PET} value of $-43\,kJ\,mol^{-1}$ and hence a facile PET process, should be virtually nonfluorescent in most common solvents.

The fluorescence spectra as well as the absorption spectra of **3**–**6** are typical of the 9-cyanoanthracene fluorophore [13]. For instance, **4** in diethyl ether solution has $\lambda_{Abs} = 410$, 388, 368 nm and $\lambda_{Flu} = 420$, 442, 467 nm. For comparison, **4** in chlorobenzene has $\lambda_{Abs} = 415$, 393, 372 nm and $\lambda_{Flu} = 428$, 450, 479 nm. In other words, the solvent effects are rather small for these parameters. However, the fluorescence quantum yield (ϕ_{Flu}) is the expected sensory parameter.

Figure 3 shows a plot of fluorescence quantum yield versus solvent polarity for compounds **3**–**6**. The mixing coefficient (k) in the solvent polarity abscissa was determined by fitting the data for **4** to Eq. (4). In this case, $k = 0.9$, $A = 2.4$, and $C = 1.6$. The other data sets for **3**, **5,** and **6** were plotted on the same graph. Compound **4**

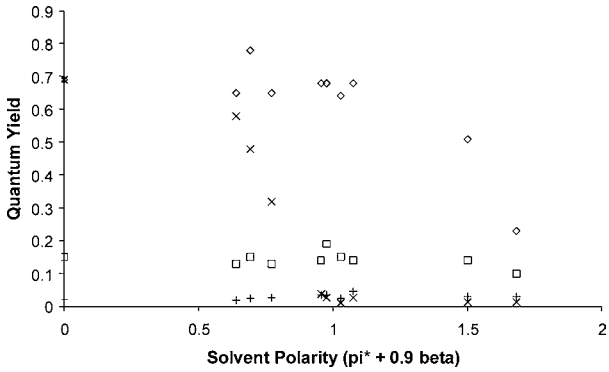

Fig. 3. Fluorescence quantum yield versus solvent polarity for probes **3–6**. (**3** = 0, **4** = x, **5** = □ , and **6** = +). The solvents (in order of increasing polarity) are: hexane, toluene, diethyl ether, chlorobenzene, ethyl acetate, methyl acetate, acetonitrile, tetrahydrofuran, dimethyl formamide, and dimethyl sulfoxide.

shows the anticipated sensory behavior, the ϕ_{Flu} value decreasing at a polarity value of 0.7. In polar media, including acetonitrile, the fluorescence of **4** is switched "off." As the solvent polarity decreases, ΔG_{PET} becomes less favorable and the fluorescence switches "on." The nonzero k value reminds us that the solvent is acting as a hydrogen bond base to engage the sensor. This can be traced to the hydrogen bond acidity of the H_3CO group in the developing dimethoxyphenyl radical cation during the PET process, even though **4** seems devoid of significant hydrogen bonding sites at first sight.

The fluorescence quantum yield of **3** remains quite high until solvents of very high polarity are employed, when the fluorescence shows clear signs of switching "off." Only in these solvents is PET sufficiently active to cause lessening of ϕ_{Flu}. Even in the most polar solvent used in this study (dimethyl sulfoxide), the fluorescence is not completely quenched. Nevertheless, the ΔG_{PET} predictions are obeyed quite accurately in the cases of **4** and **3**. These two compounds are clear cases of successful, predictive examples of amine-free sensors for solvent polarity.

The ϕ_{Flu} values for **5** and **6** remain relatively constant throughout the polarity range investigated. ΔG_{PET} calculations predicted this for **6** but not for **5**. Hence the ϕ_{Flu} values for **6** are all very small, at least partly because of the very negative ΔG_{PET} in acetonitrile. The deviant behavior of **5** can again be attributed to the anthracen-9-ylmethyloxy unit. As with Ca^{2+} sensor **2**, one of the oxygen atoms' lone pair is conjugated throughout the delocalized π system at a given moment, while the other is not. This means that two possible pathways are available for excited state deactivation: PET and CT. The highly charge-separating PET mechanism is solvent-dependent as discussed above, but the CT pathway is much less so. Therefore, the degree of CT will be virtually the same in any solvent irrespective of its polarity, leading to a nearly constant ϕ_{Flu} for **5** (and **6**).

CONCLUSION

It has been clear for a long time that inserting a single carbon atom (with its attendant hydrogens) between an electron donor and a fluorophore changes an ICT/PCT sensor into a PET sensor with qualitatively different characteristics. Now we find that inserting a single oxygen atom between an electron donor and an anthracen-9-ylmethyl system significantly attenuates the efficiency of PET sensing, whether it concerns chemical species or physical properties. What a difference an atom makes.

ACKNOWLEDGMENTS

We appreciate the help and support of EPSRC, DEL, Invest NI (RTD COE 40), and EC (HPRN-CT-2000-00029).

REFERENCES

1. A. J. Bryan, A. P. de Silva, S. A. de Silva, R. A. D. D. Rupasinghe, and K. R. A. S. Sandanayake (1989). Photoinduced electron-transfer as a general design logic for fluorescent molecular sensors for cations. *Biosensors* **4**, 169–179.
2. (a) R. A. Bissell, A. P. de Silva, H. Q. N. Gunaratne, P. L. M. Lynch, G. E. M. Maguire, and K. R. A. S. Sandanayake (1992). Molecular fluorescent signaling with "fluor–spacer–receptor" systems— approaches to sensing and switching devices via supramolecular photophysics. *Chem. Soc. Rev.* **21**, 187–195; (b) R. A. Bissell, A. P. de Silva, H. Q. N. Gunaratne, P. L. M. Lynch, G. E. M. Maguire, C. P. McCoy, and K. R. A. S. Sandanayake (1993). Fluorescent PET (photoinduced electron-transfer) sensors. *Top. Curr. Chem.* **168**, 223–264; (c) A. W. Czarnik (1994). Chemical communication in water using fluorescent chemosensors. *Acc. Chem. Res.* **27**, 302–308; (d) L. Fabbrizzi and A. Poggi (1995). Sensors and switches from supramolecular chemistry. *Chem. Soc. Rev.* **24**, 197–202; (e) A. P. de Silva, H. Q. N. Gunaratne, T. Gunnlaugsson, A. J. M. Huxley, C. P. McCoy, J. T. Rademacher, and T. E. Rice (1997). Signaling recognition events with fluorescent sensors and switches. *Chem. Rev.* **97**, 1515–1566; (f) H. Kojima and T. Nagano (2000). Fluorescent indicators for nitric oxide. *Adv. Mater.* **12**, 763–769; (g) K. Rurack (2001). Flipping the light switch "ON"—the design of sensor molecules that show cation-induced fluorescence enhancement with heavy and transition metal ions. *Spectrochim. Acta A* **57**, 2161–2195; (h) K. Rurack and U. Resch-Genger (2002). Rigidization, preorientation, and electronic decoupling—the "magic triangle" for the design of highly efficient fluorescent sensors and switches. *Chem. Soc. Rev.* **31**, 116–127; (i) R. Martinez-Manez and F. Sancenon (2003). Fluorogenic and chromogenic chemosensors and reagents for anions. *Chem. Rev.* **103**, 4419–4476. (j) J. F. Callan, A. P. de Silva, and D. C. Magri (2005). Luminescent sensors and switches in the 21st century. *Tetrahedron* **61**, 8551–8588.

3. (a) A. W. Czarnik (Ed.) (1993). *Fluorescent Chemosensors of Ion and Molecule Recognition*, ACS Symposium Series 538, American Chemical Society, Washington, DC; (b) A. W. Czarnik and J.-P. Desvergne (Eds.) (1997). *Chemosensors of Ion and Molecule Recognition*, Kluwer, Dordrecht, The Netherlands; (c) J. R. Lakowicz (1999). *Principles of Fluorescence Spectroscopy*, 2nd ed., Plenum, New York; (d) B. Valeur (2001). *Molecular Fluorescence*, Wiley-VCH, Germany. Weinheim; (e) V. Balzani, M. Venturi, and A. Credi (2003). *Molecular Devices and Machines*, Wiley-VCH, Weinheim, Germany.
4. S. C. Burdette, G. K. Walkup, B. Spingler, R. Y. Tsien, and S. J. Lippard (2001). Fluorescent sensors for Zn^{2+} based on a fluorescein platform: Synthesis, properties, and intracellular distribution. *J. Am. Chem. Soc.* **123**, 7831–7841; H. R. He, M. A. Mortellaro, M. J. P. Leiner, S. T. Young, R. J. Fraatz, and J. K. Tusa (2003). A fluorescent chemosensor for sodium based on photoinduced electron transfer. *Anal. Chem.* **75**, 549–555; H. R. He, M. A. Mortellaro, M. J. P. Leiner, R. J. Fraatz, and J. K. Tusa (2003). A fluorescent sensor with high selectivity and sensitivity for potassium in water. *J. Am. Chem. Soc.* **125**, 1468–1469; E. M. Nolan and S. J. Lippard (2003). A "Turn-On" fluorescent sensor for the selective detection of mercuric ion in aqueous media. *J. Am. Chem. Soc.* **125**, 14270–14271; X. Guo, X. Qian, and L. Jia (2004). A highly selective and sensitive fluorescent chemosensor for Hg^{2+} in neutral buffer aqueous solution. *J. Am. Chem. Soc.* **126**, 2272–2273.
5. (a) A. P. de Silva, H. Q. N. Gunaratne, J.-L. Habib-Jiwan, C. P. McCoy, T. E. Rice, and J.-P. Soumillion (1995). New fluorescent model compounds for the study of photoinduced electron-transfer—the influence of a molecular electric-field in the excited-state. *Angew. Chem. Int. Ed. Engl.* **34**, 1728–1731; (b) A. P. de Silva and T. E. Rice (1999). A small supramolecular system which emulates the unidirectional, path-selective photoinduced electron transfer (PET) of the bacterial photosynthetic reaction centre (PRC). *Chem. Commun.* 163–164.
6. A. P. de Silva, A. Goligher, H. Q. N. Gunaratne, and T. E. Rice (2003). The pH-dependent fluorescence of pyridylmethyl-4-amino-1,8-naphthalimides. *ARKIVOC*, 229–243.
7. Y. Q. Gao and R. A. Marcus (2002). Theoretical investigation of the directional electron transfer in 4-aminonaphthalimide compounds. *J. Phys. Chem. A* **106**, 1956–1960.
8. R. A. Bissell, A. P. de Silva, W. T. M. L. Fernando, S. T. Patuwathavithana, and T. K. S. D. Samarasinghe (1991). Fluorescent PET (photoinduced electron-transfer) indicators for solvent polarity with quasi-step functional-response. *Tetrahedron Lett.* **32**, 425–428.
9. A. P. de Silva and K. R. A. S. Sandanayake (1991). Fluorescent PET (photoinduced electron-transfer) sensors for alkali cations—optimization of sensor action by variation of structure and solvent. *Tetrahedron Lett.* **32**, 421–424.
10. A. P. de Silva and H. Q. N. Gunaratne (1990). Fluorescent PET (photoinduced electron-transfer) sensors selective for submicromolar calcium with quantitatively predictable spectral and ion-binding properties. *J. Chem. Soc., Chem. Commun.* 186–187.
11. G. Grynkiewicz, M. Poenie, and R. Y. Tsien (1985). A new generation of Ca^{2+} indicators with greatly improved fluorescence properties. *J. Biol. Chem.* **260**, 3440–3450.
12. M. Bullpitt, W. Kitching, D. Doddrell, and W. Adcock (1976). Substituent effect of bromomethyl group—C-13 magnetic-resonance study. *J. Org. Chem.* **41**, 760–766.
13. J. B. Birks (1970). *Photophysics of Aromatic Molecules,* Wiley, London.
14. R. Y. Tsien (1980). New calcium indicators and buffers with high selectivity against magnesium and protons—design, synthesis, and properties of prototype structures. *Biochemistry* **19**, 2396–2404.
15. A. P. de Silva, H. Q. N. Gunaratne, and P. L. M. Lynch (1995). Luminescence and charge-transfer. 4. "On-off" fluorescent PET (photoinduced electron-transfer) sensors with pyridine receptors—1,3-diaryl-5-pyridyl-4,5-dihydropyrazoles. *J. Chem. Soc. Perkin Trans.* **2**, 685–690.
16. J. R. Jefferson, J. B. Hunt, and A. Ginsburg (1990). Characterization of indo-1 and quin-2 as spectroscopic probes for Zn^{2+}-protein interactions. *Anal. Biochem.* **187**, 328–336.
17. D. Atar, P. H. Backx, M. M. Appel, W. D. Gao, and E. Marban (1995). Excitation–transcription coupling mediated by zinc influx through voltage-dependent calcium channels. *J. Biol. Chem.* **270**, 2473–2477.
18. A. Weller (1968). Electron-transfer and complex formation in the excited state. *Pure Appl. Chem.* **16**, 115–123; D. Rehm and A. Weller (1970). Kinetics of fluorescence quenching by electron and H-atom transfer. *Isr. J. Chem.* **8**, 259–269.
19. (a) H. Siegerman (1975). in N. L. Weinberg (Ed.), *Techniques of Electroorganic Synthesis – Part II*, Wiley, New York, p. 667; C. K. Mann and K. K. Barnes (1970). *Electrochemical Reactions in Non-Aqueous Systems*, Dekker, New York; (b) Z. R. Grabowski and J. Dobkowski (1983). Twisted intramolecular charge-transfer (TICT) excited-states—energy and molecular-structure. *Pure Appl. Chem.* **55**, 245–252.
20. H. Kawai, T. Nagamura, T. Mori, and K. Yoshida (1999). Picosecond mechanism of metal-ion-sensitive fluorescence of phenylimidazoanthraquinone with azacrown. *J. Phys. Chem. A* **103**, 660–664.
21. A. Castellan, J.-M. Lacoste, and H. Bouas-Laurent (1979). Study of nonconjugated bichromophoric systems, the so-called jaw photochromic materials. 1. Photocyclomerization and fluorescence of bis-9-anthrylmethyl ethers. *J. Chem. Soc., Perkin Trans.* **2**, 411–419.
22. S. Iwata, H. Matsuoka, and K. Tanaka (1997). Alkaline earth metal-sensing anthracene fluorophore-hosts. *J. Chem. Soc., Perkin Trans.* **1**, 1357–1360.
23. J.-P. Desvergne, N. Bitit, A. Castellan, H. Bouas-Laurent, and J. C. Soulignac (1987). Kinetic and thermodynamic studies on new intramolecular mixed excimers in anthracene phenanthrene and anthracene pyrene linked systems. *J. Lumin.* **37**, 175–181.
24. C. Reichardt (1994). Solvatochromic dyes as solvent polarity indicators. *Chem. Rev.* **94**, 2319–2358.
25. (a) K. Kalyanasundaram and J. K. Thomas (1977). Solvent-dependent fluorescence of pyrene-3-carboxaldehyde and its applications in estimation of polarity at micelle–water interfaces. *J. Phys. Chem.* **81**, 2176–2180; (b) R. M. Hermant, N. A. C. Bakker, T. Scherer, B. Krijnen, and J. W. Verhoeven (1990). Systematic study of a series of highly fluorescent rod-shaped donor–acceptor systems. *J. Am. Chem. Soc.* **112**, 1214–1221; (c) A. Jacobsen, A. Petric, D. Hogenkamp, A. Sinur, and J. R. Barrio (1996). 1, 1-dicyano-2-[6-(dimethylamino)naphthalen-2-yl]propene (DDNP): A solvent polarity and viscosity sensitive fluorophore for fluorescence microscopy. *J. Am. Chem. Soc.* **118**, 5572–5579.
26. M. J. Kamlet, J.-L. M. Abboud, and R. W. Taft (1981). An examination of linear salvation energy relationships. *Prog. Phys. Org. Chem.* **13**, 485–630.
27. M. D. P. de Costa, A. P. de Silva, and S. T. Pathirana (1987). 2-dimensional fluorescent sensors—the different dependences of the fluorescence band position and the fluorescence quantum yield of 1,5-diphenyl-3-vinyl-delta-2-pyrazoline upon solvent dipolarity and hydrogen-bond acidity. *Can. J. Chem.* **65**, 1416–1419.
28. M. A. Winnik and D. C. Dong (1984). The Py scale of solvent polarities. *Can. J. Chem.* **62**, 2560–2565; W. E. Acree, D. C. Wilkins, S. A. Tucker, J. M. Griffin, and J. R. Powell (1994). Spectrochemical investigations of preferential solvation. 2. Compatibility of thermodynamic models versus spectrofluorometric probe methods for tautomeric solutes dissolved in binary-mixtures. *J. Phys. Chem.* **98**, 2537–2544; N. Barrash-Shiftan, B. Brauer, and E. Pines (1998). Solvent dependence of pyranine fluorescence and UV-visible absorption spectra. *J. Phys. Org. Chem.* **11**, 743–750; B. Strehmel, A. M. Sarker, J. H. Malpert, V. Strehmel, H. Seifert, and D. C. Neckers (1999). Effect of aromatic ring substitution on the optical properties, emission dynamics, and solid-state behavior of fluorinated oligophenylenevinylenes. *J. Am. Chem. Soc.* **121**, 1226–1236.